Mechanical Systems and Signal Processing 112 (2018) 22–30

Contents lists available at ScienceDirect

Mechanical Systems and Signal Processing

journal homepage: www.elsevier.com/locate/ymssp

Output feedback in the design of eigenstructures for enhanced sensitivity

D. Bernal [a,*], M.D. Ulriksen [b]

[a] Civil and Environmental Engineering, Center for Digital Signal Processing, Northeastern University, Boston, MA, United States
[b] Department of Civil Engineering, Aalborg University, 6700 Esbjerg, Denmark

ARTICLE INFO

Article history:
Received 7 February 2018
Received in revised form 9 April 2018
Accepted 15 April 2018
Available online 22 April 2018

Keywords:
Output feedback
Sensitivity
Pole placement
Stability
Latent vectors

ABSTRACT

The problem of closed-loop enhanced sensitivity design is as follows: given a linear, time-invariant system, find a (realizable) feedback gain such that (1) the closed-loop is stable in the reference and the potentially damaged states, and (2) the eigenstructure includes a subset of poles, with desirable derivatives, that lie in a part of the plane where identification is feasible. For state feedback the eigenstructure is typically assignable and stability in the reference state is easily enforced. For output feedback, however, only partial assignment is possible, and it is here shown that the standard SVD design scheme leads to generically unstable eigenstructures when measurands are homogeneous (that is, when all sensors measure displacements, velocities, or accelerations). The mechanics that govern this behavior are clarified and a mitigating strategy that retains the convenience of homogeneous sensing is offered.

1. Introduction

Eigenstructure assignment is a control design scheme where objectives are attained by directly specifying closed-loop poles and eigenvectors [1]. The topic of this paper is eigenstructure assignment using output feedback when the purpose of the assignment is the realization of pole sensitivities favorable for Structural Health Monitoring (SHM) purposes [2–4]. A difficulty in designing for this objective derives from the fact that output feedback allows only partial control of the eigenstructure and that little can be said about where the poles that are not directly assigned end up [5]. The foregoing would not be an important issue if instability was encountered sporadically in the search for suitable gain, but results show that this is not so. Instead, what is found is that in the common case where measurands are homogeneous, that is, when all sensors are of the same type, instability in the optimization search is the norm, not the exception.

The reason why homogeneous sensing enters the problem is best appreciated in the derivations, but it can be outlined qualitatively from the outset and we do so next. Namely, in the typical (and most convenient) parameterization the gain is computed as the product of two matrices where one is the inverse of a matrix, $\boldsymbol{\Psi}$, that lists, at the measured coordinates, the right-side eigenvectors of the placed poles of the closed-loop transition matrix. The eigenvectors of the first order formulation can be written as $\psi_j = \left\{ \boldsymbol{\varphi}_j \quad \boldsymbol{\varphi}_j \lambda_j \right\}^T$, where $\boldsymbol{\varphi}_j$ is the latent vector of the second-order formulation, and since the gain is real, the columns of $\boldsymbol{\Psi}$ come in complex conjugate pairs. The issue arises because, for homogeneous measurements, all the entries in the columns of $\boldsymbol{\Psi}$ come from the top, or the bottom partition, of the eigenvectors and are, therefore, from the

* Corresponding author.
E-mail address: bernal@neu.edu (D. Bernal).

https://doi.org/10.1016/j.ymssp.2018.04.032
0888-3270/

latent vector. The latent vector is nearly real in the open loop (exactly real if the damping is assumed classical), and while this is not so in the closed loop, since the system is no longer self-adjoin, the coherence between the real and the imaginary parts is generally high. High coherence translates into poor conditioning; which implies a high norm of the inverse of $\boldsymbol{\Psi}$, hence resulting in large feedback gains and, as such, in large movements of the unplaced poles that, with near certainty, lead to instability. A solution that suggests itself is to use sensors such that the columns in $\boldsymbol{\Psi}$ contain entries from the displacement and velocity partitions of the eigenvectors, and numerical examination shows that this approach does mitigate instability. Analysis also reveals, however, that a mixed sensing scheme is not the ideal solution; not just because it is less desirable from a practical perspective, but because it does not offer a convenient means to affect the critical point, namely, the tradeoff between sensitivity and stability.

The pole placement problem by output feedback has long been known to be nonlinear in nature and it remains, in spite of significant progress, only partially solved [5–8]. In particular, it is known that for $n \leqslant m \cdot r$, where m, r, and n are the number of outputs, inputs and the system order, the system is pole assignable, although no effective algorithm to determine a gain that attains a given desired eigenstructure is available. For $n > m \cdot r$, some eigenstructures can be realized and others cannot, and it is not known how to distinguish between them; what is known, and for which there is an effective algorithm, is how to find a gain that places m poles with right-side eigenvector amplitudes generically fixed at r locations or r poles with left-side eigenvectors fixed at m locations [9,10]. Also available is a scheme that trades flexibility in the placement of r eigenvectors to allow placement of $m + r - 1$ poles [11]. Note that inasmuch as pole derivatives depend on the right- and left-side eigenvectors, design for sensitivity is an eigenstructure assignment problem, not just a pole placement one. Needless to say, the literature on the use of output feedback for stabilization, tracking, or regulation of linear systems is extensive and a survey can be found in [12]. References on its use in the control of nonlinear systems can be found in [13,14], among others.

The rest of the paper is organized as follows: following this introduction, the standard SVD eigenstructure design scheme and the computation of the closed-loop eigenvalue derivatives are reviewed. The next section clarifies the behavior that leads to ubiquitous instability for homogeneous sensing and puts forth a solution that retains the option of equal sensor types. A numerical example and a brief concluding section close the paper.

2. Pole and eigenvector placement using output feedback

Consider a linear, time-invariant system in discrete time described by

$$\boldsymbol{x}_{k+1} = \boldsymbol{A}_d\boldsymbol{x}_k + \boldsymbol{B}_d\boldsymbol{u}_k + \boldsymbol{B}_f\boldsymbol{f}_k \tag{1}$$

$$\boldsymbol{y}_k = \boldsymbol{C}\boldsymbol{x}_k \tag{2}$$

operating under the influence of static output feedback of the form

$$\boldsymbol{u}_k = -\boldsymbol{G}\boldsymbol{y}_k \tag{3}$$

Here, $\boldsymbol{x}_k \in \Re^{n\times 1}$ is the state, $\boldsymbol{y}_k \in \Re^{m\times 1}$ is the output, $\boldsymbol{u}_k \in \Re^{r\times 1}$ are the control inputs, and $\boldsymbol{f}_k \in \Re^{z\times 1}$ is the exogenous loading, which may be stochastic, if from ambient sources, or deterministic, if actuators are used to deliver it. $\boldsymbol{G} \in \Re^{r\times m}$ is the controller gain while $\boldsymbol{A}_d \in \Re^{n\times n}$, $\boldsymbol{B}_d \in \Re^{n\times r}$, $\boldsymbol{B}_f \in \Re^{n\times z}$ and $\boldsymbol{C} \in \Re^{m\times n}$ are the system matrices, and we assume throughout that $\{\boldsymbol{A}_d, \boldsymbol{B}_d\}$ is controllable and $\{\boldsymbol{A}_d, \boldsymbol{C}\}$ is observable. Eq. (2) holds directly when measurements are displacements, velocities, or non-collocated accelerations and can be used in the case of collocated accelerations if the direct transmission matrix is known and its contribution is subtracted from the measurements. Substituting Eq. (2) into Eq. (1) one finds that the closed-loop system is

$$\boldsymbol{x}_{k+1} = (\boldsymbol{A}_d - \boldsymbol{B}_d\boldsymbol{G}\boldsymbol{C})\boldsymbol{x}_k + \boldsymbol{B}_f\boldsymbol{f}_k \tag{4}$$

Let, $\Lambda = \{\lambda_1 \quad \cdots \quad \lambda_p\}$ be the location of p closed-loop poles. For $\boldsymbol{G}$, to be real, Λ must be closed under conjugation, and it is evident that a necessary condition for stability is $\|\lambda_j\| \leqslant 1$. Since the controller is implemented in discrete time (DT), it is appropriate to extract the gain operating in DT so that the effect of the inter-sample behavior of the control can be considered [15]. The closed-loop eigenvalue problem writes

$$(\boldsymbol{A}_d - \boldsymbol{B}_d\boldsymbol{G}\boldsymbol{C})\boldsymbol{\psi}_j = \boldsymbol{\psi}_j\lambda_j \tag{5}$$

from where

$$[\boldsymbol{A}_d - \boldsymbol{I}\cdot\lambda_j \quad -\boldsymbol{B}_d]\begin{Bmatrix}\boldsymbol{\psi}_j \\ \boldsymbol{G}\boldsymbol{C}\psi_j\end{Bmatrix} = \boldsymbol{0} \tag{6}$$

Defining

$$\boldsymbol{V}_j = Null([\boldsymbol{A}_d - \boldsymbol{I}\cdot\lambda_j \quad -\boldsymbol{B}_d]) = \begin{bmatrix}\boldsymbol{S}_j \\ \boldsymbol{Q}_j\end{bmatrix} \tag{7}$$

where *Null* indicates the null space of the matrix in parenthesis and, assuming full row rank, $\boldsymbol{S}_j \in \mathbb{C}^{n\times r}$ and $\boldsymbol{Q}_j \in \mathbb{C}^{r\times r}$ and it follow that

$$\begin{bmatrix} \boldsymbol{S}_j \\ \boldsymbol{Q}_j \end{bmatrix} \{\theta_j\} = \begin{Bmatrix} \boldsymbol{\psi}_j \\ \boldsymbol{b}_j \end{Bmatrix} \tag{8}$$

where θ_j are arbitrary constants (except for the fact that they must be conjugates for conjugate poles) and it is clear that we've defined

$$\boldsymbol{b}_j = \boldsymbol{GC}\boldsymbol{\psi}_j \tag{9}$$

Taking

$$\boldsymbol{\Psi} = \boldsymbol{C}\cdot\begin{bmatrix} \boldsymbol{\psi}_1^{CL} & \cdots \boldsymbol{\psi}_p^{CL} \end{bmatrix} \text{ and } \boldsymbol{\Gamma} = \begin{bmatrix} \boldsymbol{b}_1 & \cdots & \boldsymbol{b}_p \end{bmatrix} \tag{10-11}$$

writes

$$\boldsymbol{G}\cdot\boldsymbol{\Psi} = \boldsymbol{\Gamma} \tag{12}$$

where $\boldsymbol{\Psi} \in \mathbb{C}^{m\times p}$ and $\boldsymbol{\Gamma} \in \mathbb{C}^{r\times p}$. Inspecting the dimensions one finds that the coefficient matrix is square when the number of placed poles equals the number of outputs and thus, on the premise that the eigenvectors have been selected so that $\boldsymbol{\Psi}$ is full rank, one has

$$\boldsymbol{G} = \boldsymbol{\Gamma}\cdot(\boldsymbol{\Psi})^{-1} \tag{13}$$

Since transposition does not change the eigenvalues it is also possible, as noted previously, to operate with left-side eigenvectors and place r poles.

3. Closed-loop pole sensitivities

Let $\boldsymbol{P}$ be a non-defective but otherwise arbitrary square matrix that is a function of some parameter, θ. We shall refer to the derivatives of the eigenvalues of $\boldsymbol{P}$ with respect to θ as sensitivities; not to be confused with the matrix in the Laplace domain that carries the same name [16]. The sensitivity of the jth eigenvalue writes

$$\lambda_j' = \boldsymbol{\varphi}_j^T \boldsymbol{P}' \boldsymbol{\psi}_j \tag{14}$$

where $\boldsymbol{\psi}_j$ and $\boldsymbol{\varphi}_j$ are the right- and left-side eigenvectors and the prime indicates differentiation with respect to θ. We now particularize Eq. (14) to the case where $\boldsymbol{P}$ is the transition matrix of a finite-dimensional, linear, time-invariant, discrete-time system under output feedback. From Eq. (4), we have that the closed-loop matrix is

$$\boldsymbol{P} = \boldsymbol{A}_d - \boldsymbol{B}_d\boldsymbol{GC} \tag{15}$$

which, noting that the gain is not a function of θ, has the derivative

$$\boldsymbol{P}' = \boldsymbol{A}_d' - \boldsymbol{B}_d'\boldsymbol{GC} - \boldsymbol{B}_d'\boldsymbol{GC}' \tag{16}$$

The relation between $\boldsymbol{B}_d$ and its continuous-time counterpart is a function of how the control action is delivered. It is common to operate on the premise that this action is applied through a D/A zero-order-hold circuit, which, when neglecting delays, leads to the relation

$$\boldsymbol{B}_d = \boldsymbol{A}_c^{-1}(\boldsymbol{A}_d - \boldsymbol{I})\boldsymbol{B}_c \tag{17}$$

with $\boldsymbol{B}_c \in \Re^{n\times r}$ being the control input-to-state matrix in continuous time. Differentiating Eq. (17) with respect to θ writes

$$\boldsymbol{B}_d' = \boldsymbol{A}_{\rm d}^{-1}(\boldsymbol{A}_d'\boldsymbol{B}_c + \boldsymbol{A}_d\boldsymbol{B}_c' - \boldsymbol{B}_c' - \boldsymbol{A}_c'\boldsymbol{B}_d) \tag{18}$$

thus Eq. (16) can be restated as

$$\boldsymbol{P}' = \boldsymbol{A}_d' - \boldsymbol{A}_c^{-1}(\boldsymbol{A}_d'\boldsymbol{B}_c + (\boldsymbol{A}_d - \boldsymbol{I})\boldsymbol{A}_d'\boldsymbol{B}_c' - \boldsymbol{A}_c'\boldsymbol{B}_d)\boldsymbol{GC} - \boldsymbol{B}_d\boldsymbol{GC}' \tag{19}$$

The open-loop transition matrix in discrete time is given by

$$\boldsymbol{A}_d = e^{\boldsymbol{A}_c\Delta t} \tag{20}$$

where Δt is the sampling time step. The derivative of Eq. (20) with respect to θ is needed to evaluate Eq. (18), and in doing so it is necessary to keep in mind that the derivative of the exponential matrix does not follow the elementary calculus rules. An efficient numerical approach uses the complex perturbation scheme [17–19] and writes

$$\boldsymbol{A}_d' = \lim_{\varepsilon\to 0}\Im\left(\frac{e^{(\boldsymbol{A}_c+\boldsymbol{A}_c'\varepsilon i)\Delta t}}{\varepsilon}\right) \tag{21}$$

where ε can be taken very small without incurring finite precision difficulties. The eigenvalue sensitivity realized in a conventional identification is a result in DT but the sensitivities that a user is reported on pole positions is typically mapped to continuous time using Eq. (20). Therefore, since

$$\lambda_c = \frac{\log(\lambda_d)}{\Delta t} \tag{22}$$

one has

$$\lambda_c' = \frac{\lambda_d'}{\lambda_d \Delta t} \tag{23}$$

and it is the result from Eq. (23) that determines the "reported" tangent to the pole path. It is worth noting that Eqs. (22) and (23) are only operational since there is no strict continuous time closed-loop eigenvalue, given that the closed loop transition matrix depends on the inter-sample behavior of the control signal.

4. Instability in SVD assignment for homogeneous measurements

Eq. (13) shows that m poles can be arbitrarily placed provided $\boldsymbol{\Psi}$ is invertible. This matrix, as previously noted, lists the right-side eigenvectors at the location of the sensors and one gathers that since these vectors come in conjugate pairs, the conditioning of $\boldsymbol{\Psi}$ depends on the degree of linear dependence between the real and the imaginary component of its columns. When measurements are all displacements, all velocities, or all accelerations, the entries in $\boldsymbol{\Psi}$ are from the latent vectors of the second-order formulation, where these are, we recall, the "eigenvectors" of the polynomial eigenvalue problem of the damped second order formulation [20]. In the closed-loop the latent vectors are complex independently of the damping, because the system is not self-adjoin [21], but, as the next subsection shows, the irreducible complexity is typically small and, as a consequence, $\boldsymbol{\Psi}$, when formed as a square matrix, is poorly conditioned. Needless to say, poor conditioning of $\boldsymbol{\Psi}$ leads to large gains, large gains lead to large movements of the unplaced poles and, with near certainty, to some poles taking unstable positions.

4.1. On the irreducible complexity of the closed loop latent vectors

This section offers support to the contention that the latent vectors in closed-loop (for typical conditions) have strongly coherent real and imaginary parts. It is shown that this contention holds quite generally for displacement and acceleration measurements, while for velocity it holds conditional on the imaginary component of the closed-loop pole in question being close to that of an open-loop one.

4.1.1. Displacement measurements

Consider the closed-loop system in second-order form. For displacement measurements, one has

$$\left(\boldsymbol{M}\lambda^2 + \boldsymbol{C}_{dam}\lambda + (\boldsymbol{K} + \boldsymbol{b}_2\boldsymbol{G}_d\boldsymbol{C}_d)\right)\boldsymbol{\varphi} = \boldsymbol{0} \tag{24}$$

where we have added the subscript "d" to indicate displacement, $\boldsymbol{b}_2 \in \Re^{dof\times r}$ is the matrix that gives the position of the actuators, and it is understood that the eigenvalue and latent vector correspond to a particular mode. Finally, we note for clarity that the positive sign in the feedback term is consistent with the negative sign used in Eq. (3), and that the matrix $\boldsymbol{C}_d \in \Re^{m\times dof}$ is the selector of the measured coordinates in the second-order formulation, not the state-to-output matrix of Eq. (2). When the measurements are velocities or accelerations we shall use the notation, $\boldsymbol{C}_v$ and $\boldsymbol{C}_a$ to refer to the selector matrices. Expressing the eigenvalue and the latent vector in terms of their real and imaginary parts writes

$$(\boldsymbol{L} + \boldsymbol{S}i)(\boldsymbol{\varphi}_R + \boldsymbol{\varphi}_I i) = \boldsymbol{0} \tag{25}$$

where

$$\boldsymbol{L} = \boldsymbol{M}(\lambda_R^2 - \lambda_I^2) + (\boldsymbol{K} + \boldsymbol{b}_2\boldsymbol{G}_d\boldsymbol{C}_d) + \boldsymbol{C}_{dam}\lambda_R \tag{26}$$

and

$$\boldsymbol{S} = 2\boldsymbol{M}\lambda_R\lambda_I + \boldsymbol{C}_{dam}\lambda_I \tag{27}$$

In the undamped case with closed-loop poles on the imaginary one has, $\boldsymbol{S} = 0$, and Eq. (25) shows that the real and the imaginary parts of the latent vector are scaled versions of the null space of $\boldsymbol{L}$ (which is of dimension one for simple poles) and are thus perfectly correlated. In the general case this is not exactly so, but inspection of Eqs. (26) and (27) shows that $\|\boldsymbol{L}\| \gg \|\boldsymbol{S}\|$ and one surmises, on a continuity argument, that the correlation between the two components of the latent vector is strong.

4.1.2. Velocity measurements

The matrices $\boldsymbol{L}$ and $\boldsymbol{S}$ are now

$$\boldsymbol{L} = \boldsymbol{M}(\lambda_R^2 - \lambda_I^2) + (\boldsymbol{K} + \boldsymbol{b}_2\boldsymbol{G}_v\boldsymbol{C}_v\lambda_R) + \mathbf{C}_{dam}\lambda_R \tag{28}$$

and

$$\boldsymbol{S} = 2\boldsymbol{M}\lambda_R\lambda_I + (\mathbf{C}_{dam} + \boldsymbol{b}_2\boldsymbol{G}_v\boldsymbol{C}_v)\lambda_I \tag{29}$$

and examination shows that the previous argument of the dominance of $\boldsymbol{L}$ over $\boldsymbol{S}$ does not hold true. One can gain some insight, however, by postulating that the latent vector can be normalized to real and examining the implications. Indeed, taking the latent vector as $\boldsymbol{q}$, Eqs. (25), (28) and (29) require that

$$\boldsymbol{M}(\lambda_R^2 - \lambda_I^2)\boldsymbol{q} + (\boldsymbol{K} + \boldsymbol{b}_2\boldsymbol{G}_v\boldsymbol{C}_v\lambda_R)\boldsymbol{q} + \mathbf{C}_{dam}\lambda_R\boldsymbol{q} = \mathbf{0} \tag{30}$$

and

$$2\boldsymbol{M}\lambda_R\boldsymbol{q} + (\mathbf{C}_{dam} + \boldsymbol{b}_2\boldsymbol{G}_v\boldsymbol{C}_v)\boldsymbol{q} = \mathbf{0} \tag{31}$$

Multiplying Eq. (31) by λ_R and substituting the result in Eq. (30) writes

$$-\boldsymbol{M}\lambda_I^2\boldsymbol{q} - \boldsymbol{M}\lambda_R^2\boldsymbol{q} + \boldsymbol{K}\boldsymbol{q} = \mathbf{0} \tag{32}$$

and, since the real part of the eigenvalue is small,

$$(\boldsymbol{K} - \boldsymbol{M}\lambda_I^2)\boldsymbol{q} \cong \mathbf{0} \tag{33}$$

From Eq. (33) one gathers that if the imaginary part of the closed-loop eigenvalue is close to the jth open loop undamped frequency then the jth undamped mode shape, which is real, is a good approximation of $\boldsymbol{q}$. In practice the noted proximity is typically realized and the latent vector proves to have strongly correlated real and imaginary parts.

4.1.3. Acceleration measurements

The matrices $\boldsymbol{L}$ and $\boldsymbol{S}$ are now

$$\boldsymbol{L} = (\boldsymbol{M} + \boldsymbol{b}_2\boldsymbol{G}_a\boldsymbol{C}_a)(\lambda_R^2 - \lambda_I^2) + \mathbf{C}_{dam}\lambda_R + \boldsymbol{K} \tag{34}$$

and

$$\boldsymbol{S} = 2(\boldsymbol{M} + \boldsymbol{b}_2\boldsymbol{G}_a\boldsymbol{C}_a)\lambda_R\lambda_I + \mathbf{C}_{dam}\lambda_I \tag{35}$$

and one can confirm that $\|\boldsymbol{L}\| \gg \|\boldsymbol{S}\|$ and thus the argument made in the case of displacement measurements holds. Numerical validation of the contentions made in this section can be found in Appendix A.

5. Solution alternatives

There are at least two ways to mitigate the ubiquitous instability that plagues the SVD assignment scheme when measurements are homogeneous. The first is, of course, to discard homogeneous sensing and use heterogeneous measurement feedback. Indeed, if, for example, some measurements are displacements and some are velocities, one has that the jth column of $\boldsymbol{\Psi}$ is

$$\begin{bmatrix} \boldsymbol{C}_d & \mathbf{0} \\ \mathbf{0} & \boldsymbol{C}_v \end{bmatrix} \cdot \begin{Bmatrix} \boldsymbol{\varphi}_j \\ \boldsymbol{\varphi}_j\lambda_j \end{Bmatrix} = \begin{Bmatrix} \boldsymbol{C}_d\boldsymbol{\varphi}_j \\ \boldsymbol{C}_v\boldsymbol{\varphi}_j\lambda_j \end{Bmatrix} \tag{36}$$

and since λ_j is complex, and is dominated by the imaginary part, the vector in Eq. (36) and its conjugate are not highly coherent. This solution, however, is not ideal for two reasons: the first is the practical matter that homogeneous sensing is a "simpler alternative", and the second, the most important, is that it does not offer a clear means to affect the tradeoff between sensitivity and stability. Recalling that the transpose of the left eigenvectors is the inverse of the right, it is evident that sensitivity is intimately connected with the conditioning of the right-side eigenvectors. If the conditioning is too poor sensitivity is too large and instability results. If, instead, the condition number is too low, substantial eigenvalue derivatives cannot be attained.

5.1. Weighted least square solution

A simple approach that retains the possibility of homogeneous sensing and allows effective control of the tradeoff between sensitivity and stability is to form $\boldsymbol{\Psi}$ using $p \geqslant 2m$, so that nearly coherent pairs of columns are no longer critical, and introduce a weighting affecting m poles. As the weights increase the least square solution approaches that when $\boldsymbol{\Psi}$ is square and instability reigns. In the unweighted solution conditioning depends on how large one takes p. Needless to say, for $p > m$ Eq. (12) is overdetermined and the gain in any given trial may or may not realize the target poles. Discrepancies between target and realized positions are not, however, particularly important since it is not the positions but the derivatives that are of interest, and these are computed for the actual realization. From Eq. (12) and the well-known weighted least squares formulation one has

$$\boldsymbol{G} = \Gamma \boldsymbol{W} \boldsymbol{\Psi}^H (\boldsymbol{\Psi} \boldsymbol{W} \boldsymbol{\Psi}^H)^{-1} \quad (37)$$

where the superscript H stands for conjugate transpose and W is the weighting matrix; which one would likely take as $\boldsymbol{W} = diag(\,\alpha \cdot 1_m \quad 1_{p-m}\,)$ where 1_j is a vector of ones with j entries, and where it is understood that $\boldsymbol{\Psi}$ is assembled using $p \geqslant 2m$ poles. In the numerical section we take $p = n$. We note in closing that the selection of α does not require "fine tuning" since good performance can be obtained over a wide range of values.

6. Numerical illustrations

The design of closed-loop eigenstructures for monitoring requires decisions on the cost function to be maximized (minimized), decisions on where to set the constraints regarding stability during interrogation, and specification of the limits that the hardware imposes on the controller. Specific choices on these items are made in this example, but the objective here is not to suggest design criteria. It is, instead, to highlight the stability issue when output feedback is selected, and how it can be effectively mitigated. The structure, depicted in Fig. 1, has 4 displacement sensors and 2 actuators, and we consider two damage distributions, loss of stiffness in level #1 or level #3. The points to be exemplified are: (a) the SVD eigenstructure design with homogeneous measurands and precise pole placement is typically unstable, (b) use of non-homogeneous measurements resolves the stability issue but restricts the sensitivity improvements, (c) a least square solution that places the full spectrum behaves similar to (b), and (d) a weighted least square solution allows convenient control of the tradeoff between sensitivity and stability.

Design is carried out as follows:

- Free parameters: $\boldsymbol{\Theta} = \{\,\theta_1 \quad \cdots \quad \theta_6\,\}$ with $\lambda_j = \theta_j \lambda_j^{OL} \quad j = 1, 2 \quad \boldsymbol{\Theta} \in \Re^{1\times 6}$ and the other 4 constants are used to collapse the eigenvector basis.
- Constraints: $\Re(\lambda_c) \leqslant 0$ for 25% damage in levels #1 or #3, and $\|\boldsymbol{G}\|_2 \leqslant 2000$, where $\boldsymbol{G}$ is the controller gain.
- Objective: $\arg\max\limits_{\boldsymbol{\Theta}} z := \{z|\min(\sigma)\}$ where $\sigma =$ singular values of the Jacobian.

In cases (a) and (b) nothing has to be said regarding the unplaced poles and in (c) and (d) we attempt to place them at the location of the open loop ones and take the constants that collapse the eigenvector bases to maximize the projection of the closed-loop eigenvectors on the corresponding open loop ones. The stability constraint considers only single damage and the limit at 25%, needless to say, is a judgement on the maximum extent that appeared reasonable to contemplate. A realistic constraint on the feedback gain requires information on the hardware. In this case the selection was made so the maximum forces appeared "reasonable" when compared to the open-loop story shears for the excitation level used.

6.1. Results

For the purpose of subsequent contrast we note that the open loop Jacobian is

$$\boldsymbol{J}^{OL} = \begin{bmatrix} 0.035i & 0.095i \\ 0.096i & 0.087i \end{bmatrix} \cdot 10^{-2}$$

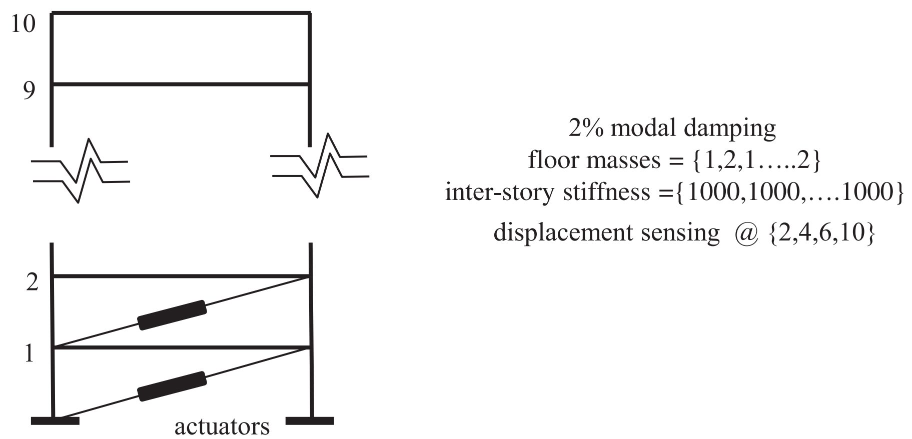

Fig. 1. Structure used for numerical illustrations.

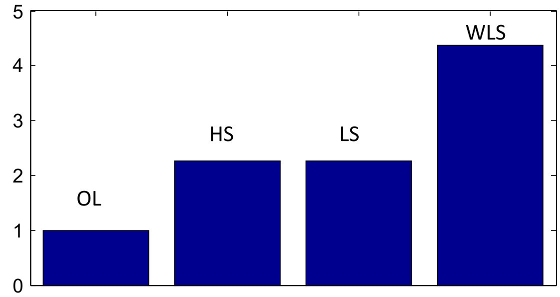

Fig. 2. Sum of the absolute values of the imaginary part of the Jacobians, normalized to the open-loop.

(a) Precise placement of 4 poles

A genetic optimization algorithm was run to search for the gain and it failed to identify any gain for which the eigenstructure proved stable.

(b) The sensors at coordinates 4 and 6 are switched from displacement to velocity

The optimization converged to

$$\boldsymbol{J}^{HS} = \begin{bmatrix} 0.002 + 0.081i & -0.006 + 0.281i \\ 0.014 + 0.263i & -0.018 - 0.061i \end{bmatrix} \cdot 10^{-2}$$

At the "optimal" solution, the 6 free parameters were $\boldsymbol{\Theta} = \{0.260, 0.878, 0.058, 0.990, 1.287, 0.008\}$ and tracking showed 1044 trials where the eigenstructure satisfied all the stability constraints and 176 where it did not. The improvement in sensitivity over the open loop is notable but not large.

(c) Least square placement of all the poles

The optimization converged to

$$\boldsymbol{J}^{LS} = \begin{bmatrix} 0.004 + 0.142i & 0.003 + 0.299i \\ -0.0005 + 0.180i & -0.004 + 0.067i \end{bmatrix} \cdot 10^{-2}$$

At the "optimal" solution, the 6 free parameters were $\boldsymbol{\Theta} = \{0.278, 0.462, 5.357, 9.864, 9.900, -1.583\}$ and tracking showed 2001 trials where the eigenstructure satisfied all the stability constraints and 19 where it did not. The performance is qualitatively the same as in the non-homogeneous sensing in (b).

(d) Weighted least square placement ($\alpha = 10^4$)

$$\boldsymbol{J}^{WLS} = \begin{bmatrix} 0.112 + 0.192i & 0.087 + 0.467i \\ -0.104 + 0.524i & -0.091 - 0.147i \end{bmatrix} \cdot 10^{-2}$$

At the "optimal" solution, the 6 free parameters were $\boldsymbol{\Theta} = \{0.253, 0.322, 0.271, 0.280, -0.474, 0.820\}$ and tracking showed 918 trials where the eigenstructure satisfied all the stability constraints and 422 where it did not.

Fig. 2 depicts the sum of the absolute value of the Jacobian entries, normalized to the result of the open loop and shows, as expected, that the performance (as viewed from this index) is best in the weighted least square option.

7. Concluding observations

The paper has shown that the standard SVD eigenstructure assignment leads to generically unstable eigenstructures for precise pole placement from output feedback when sensors measure the same quantities. The issue proves to be ultimately one of controlling the conditioning of the right-side eigenvector matrix that needs to be "inverted" to solve for the gain. If the conditioning is too poor generic instability results, but if it is too low improvements in sensitivity are marginal. It is shown that a weighted least square solution, where the full spectrum is "placed" with high weights assigned to a number of poles equal to the number of sensors, provides a convenient means to control the trade-off between sensitivity and stability.

Acknowledgements

This research was funded by NSF grant 1634277 "Monitoring the Health of Structural Systems from the Geometry of Sensor Traces", this support is gratefully acknowledged.

Appendix A. On the inherent complexity of the closed-loop latent vectors (numerical validation)

We consider a 4-dof shear building with $\boldsymbol{m} = \{1, 2, 1, 2\}$, $\boldsymbol{k} = \{1, 1, 1, \} \cdot 500$ and 5% modal damping. Actuators are placed in levels 1 and 2 and sensors in levels 3 and 4. The feedback gains are selected using the unweighted least squares scheme taking p = 8 (the system order) and $\boldsymbol{\Lambda} = 0.85\boldsymbol{\Lambda}^{OL}$ with the latent vectors obtained by taking the constants in Eq. (8) equal to one. The results are as follows:

Displacement measurements

$$\boldsymbol{G}_d = \{\, 2914.7 \quad -926.4 \,\} \quad \|\boldsymbol{L}\| = 3184.1 \quad \|\boldsymbol{S}\| = 21.7$$

confirming the contention $\|\boldsymbol{L}\| \gg \|\boldsymbol{S}\|$. The pole with the lowest frequency and the associated latent vector are:

$$\lambda = -0.259 + 5.178i \qquad \boldsymbol{\varphi} = \left\{ \begin{array}{c} 0.21 \\ 0.41 + 0.0001i \\ 0.56 + 0.0005i \\ 0.69 + 0.0013i \end{array} \right\}$$

clearly showing that the latent vector is nearly normalizable to real.

Velocity measurements

In this case the results are

$$\boldsymbol{G}_v = \{\, -12398 \quad 3785 \,\} \quad \|\boldsymbol{L}\| = 3466.9 \quad \|\boldsymbol{S}\| = 67121.1$$

Confirming that the argument based on the norm of **L** and **S** does not apply. The latent vector associated with the lowest frequency pole is the same as when measuring displacements. The undamped frequency closest to the closed loop value is 6.09 and the associated open loop undamped vector is

$$\boldsymbol{\phi}_1 = \left\{ \begin{array}{c} 0.21 \\ 0.40 \\ 0.54 \\ 0.63 \end{array} \right\}$$

which can be seen to be close to the realized latent vector. To further confirm the validity of the contention regarding the required proximity of the closed loop pole to an undamped one we redesigned the closed loop by shifting the poles to $\boldsymbol{\Lambda} = 0.5\boldsymbol{\Lambda}^{OL}$ and get

$$\boldsymbol{G}_v = \{\, -2.92 \quad 0.78 \,\} \cdot 10^4 \quad \|\boldsymbol{L}\| = 0.12e^6 \quad \|\boldsymbol{S}\| = 1.1e^6$$

with the lowest frequency pole and the associated latent vector as

$$\lambda = -0.153 + 3.046i \quad \boldsymbol{\varphi} = \left\{ \begin{array}{c} 0.19 \\ -0.095 + 0.1556i \\ -0.173 - 0.6379i \\ 0.703 - 0.0052i \end{array} \right\}$$

which is now strongly complex.

Acceleration measurements

The results are

$$\boldsymbol{G}_a = \{\, -139.2 \quad 126.6 \,\} \quad \|\boldsymbol{L}\| = 4929.6 \quad \|\boldsymbol{S}\| = 503.0$$

confirming that $\|\boldsymbol{L}\| > \|\boldsymbol{S}\|$. The latent vector for the pole with lowest frequency (for the $\boldsymbol{\Lambda} = 0.85\boldsymbol{\Lambda}^{OL}$ design) is:

$$\boldsymbol{\varphi} = \left\{ \begin{array}{c} 0.24 \\ 0.41 + 0.0003i \\ 0.57 + 0.0009i \\ 0.63 + 0.0016i \end{array} \right\}$$

which, as before, is nearly real.

References

[1] G.P. Liu, R.J. Patton, Eigenstructure Assignment for Control System Design, John Wiley & Sons, Chichester, 1998.
[2] L. Ray, L. Tian, Damage detection in smart structures through sensitivity enhancing feedback control, J. Sound Vib. 227 (5) (1999) 987–1002.
[3] B.H. Koh, L.R. Ray, Feedback controller design for sensitivity-based damage localization, J. Sound Vib. 273 (1) (2004) 317–335.
[4] L.J. Jiang, J.J. Tang, K.W. Wang, An optimal sensitivity-enhancing feedback control approach via eigenstructure assignment for structural damage identification, J. Vib. Acoust. 129 (6) (2007) 771–783.
[5] H. Kimura, Pole assignment by output feedback: a long standing open problem, in: Proceedings of the 33rd Conference on Decision and Control, Lake Buena Vista FL, 1994, pp. 2101–2105.
[6] V.L. Syrmos, C. Abdallah and P. Dorato, Static output feedback: A survey, Proceedings of the 33rd Conference on Decision and Control, Lake Buena Vista FL (1994) 837-842.
[7] B.-H. Kwon, M.-J. Youn, Eigenvalue-generalized eigenvector assignment by output feedback, IEEE Trans. Autom. Control 32 (5) (1987) 417–421.
[8] J. Rosenthal, J.C. Willems, Open problems in the area of pole placement, in: V. Blondel, E.D. Sontag, M. Vidyasagar, J.C. Willems (Eds.), Open Problems in Mathematical Systems and Control Theory, 1999, pp. 181–191.
[9] T.B. Cunningham, Eigenspace selection procedures for closed loop response shaping with modal control, in: 19th IEEE Conference on Decision and Control including the Symposium on Adaptive Processes, 1980, pp. 178–186.
[10] C.I. Byrnes, Pole assignment by output feedback, in: H. Nijmeijer, J.M.Schumacher (Eds.), Three Decades of Mathematical System Theory, ser. Lecture Notes in Control and Information Sciences #135, Springer–Verlag, 1989, pp. 31–78.
[11] S. Srinathkumar, Eigenvalue/eigenvector assignment using output feedback, NASA Technical Paper 1118, 1978.
[12] V.L. Syrmos, C. Abdallah, P. Dorato, K. Grigoriadis, Static output feedback: a survey, 1995, <http://digitalrepository.unm.edu/ece_rpts/10>.
[13] A. Isidori, Nonlinear Control Systems, third ed., Springer-Verlag, London, 1995.
[14] A. Isidori, Nonlinear Control Systems II, first ed., Springer-Verlag, London, 1999.
[15] D. Bernal, Eigenvalue sensitivity of sampled time systems operating in closed loop, Mech. Syst. Signal Process. 105 (2018) 481–487.
[16] W.L. Brogan, Modern Control Theory, third ed., Prentice Hall, 1991.
[17] J.N. Lyness, C.B. Moler, Numerical differentiation of analytic functions, SIAM J. Numer. Anal. 4 (2) (1967) 202–210.
[18] G.M. Tuynman, The derivation of the exponential map of matrices, Am. Math. Mon. 102 (9) (1995) 818–820.
[19] D. Bernal, Sensitivities of eigenvalues and eigenvectors from complex perturbations, in: Topics in Modal Analysis II, Volume 6: Proceedings of the 30th IMAC, A Conference on Structural Dynamics, 2012, pp. 589–593.
[20] E. Balmes, New results on the identification of normal modes from experimental complex modes, Mech. Syst. Signal Process. 11 (2) (1997) 229–243.
[21] Q. Zhang, G. Lallement, R. Fillod, Relations between the right and left eigenvectors of non-symmetric structural models. Applications to rotors, Mech. Syst. Signal Process. 2 (1) (1988) 97–103.